Macromolecules

ARTICLE

pubs.acs.org/Macromolecules

Formation of Nano-/Microstructures of Polyaniline and its Derivatives

Chunhua Luo,[†] Hui Peng,[*,†] Lijuan Zhang,[‡] Guo-Liang Lu,[§] Yiting Wang,[†] and Jadranka Travas-Sejdic[*,‡,⊥]

[†]Key Laboratory of Polarized Materials and Devices, Ministry of Education, East China Normal University, Shanghai 200062, China

[‡]Polymer Electronic Research Centre, The University of Auckland, Auckland, New Zealand

[§]Auckland Cancer Society Research Centre, The University of Auckland, Auckland, New Zealand

[⊥]MacDiarmid Institute for Advanced Materials and Nanotechnology, Wellington, New Zealand

ABSTRACT: In this work, we systematically investigated the morphologies of polymers prepared by chemical oxidation of aniline and methyl-, methoxy-, or ethoxy-substituted aniline under the same experimental conditions. No matter the presence or absence of 10-camphorsulfonic acid (CSA), the oxidation of aniline produces nanotubes, while the oxidation of most aniline derivatives produce hollow microspheres under the same experimental conditions. These results illustrate the oligomers with phenazine-like structures produced at the initial oxidation of aniline are crucial for the formation of PANI nanotubes. The formation mechanism of the hollow microspheres of PANI derivatives is discussed. The main factors to control the polymer morphology are stability of droplets of aniline and its derivatives formed in an aqueous solution and the rate of exothermal reaction. The fast exothermal reaction benefits the formation of uniform microspheres. We also suggest that the hole on the surface of microspheres forms at the initial oxidation stage and is maintained by the flux of water and water-soluble components in the course of polymerization.

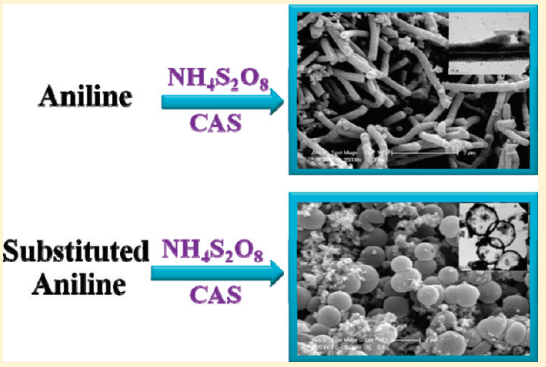

INTRODUCTION

Since the observation of the remarkably high electrical conductivity of a halogen-treated polyacetylene,[1] a number of other conjugated polymers have shown transition from an insulating into a highly conductive state, such as polyaniline (PANI), poly(phenylenevinylene), polypyrrole, and polythiophene. Because of their unique electrical properties covering the whole insulator-semiconductor-metal range, unusual conducting mechanism and controllable chemical and electrochemical properties, conducting polymers show not only great potential in a range of applications, but also great contribution to the fundamental materials science research. With the development of nanotechnology in recent years, conducting polymer nanostructures have been receiving more and more attention because they can act as excellent molecular wires in nanodevices due to their highly π-conjugated polymeric chains and metal-like conductivity.[2]

Among conducting polymers, PANI nanotubes/nanowires have been widely studied. Different approaches including hard template method, self-assembly method and electrospinning are used to synthesize or fabricate PANI nanotubes/nanowires and their composite nanostructures.[2−5] Among these approaches, the self-assembly method first reported by Wan's group[6] has the advantage in preparing PANI nanostructures of being simple and low cost.[7] In this method, "structure directors", such as surfactants[8] or polyelectrolytes[5] are introduced into the chemical polymerization solution as dopants. In the course of chemical polymerization PANI nano-/microtubes can be obtained. Large efforts have been made to investigate the effect of the experimental conditions such as the concentrations and molar ratio of dopant, oxidant and monomer, pH values of polymerization solution, reaction time, temperature, etc. on the morphology of PANI nano/micro- structures prepared by self-assembly method.[4,7,9,10] For example, Wan's group found that hollow microspheres of PANI could be changed into nanotubes by varying either the polymerization temperature[11] or the molar ratio of dopant to aniline.[12] The diameter of the nanostructures was also related to the size and concentration of dopant, which increases with the increase of dopant concentration and the molar ratio of dopant to aniline.[12,13]

However, the formation mechanism of self-assembly of PANI nano/microtubes is still not well understood. Wang's group proposed a formation mechanism of nanotubes which assumes the existence of cylindrical micelles of aniline salts with organic acids as a specific soft templates.[14] In the beginning of polymerization, such templates acted as a skeleton for the growth of the nanotubular walls and are gradually consumed during the polymer chain growth, leaving the cavity inside.[14] In this proposed mechanism, the existence of micelles is essential for the formation of nanotubes, but it has not been clearly proved and how these micelles assemble to tubular skeleton is still in question. Moreover, PANI nanotubes are also produced in the presence of low concentration of inorganic acids[13] which do not produce micelles or insoluble salts with aniline[9,15,16] or even without any acid.[17,18] Stejskal et al[15,19−21] proposed the precipitate of aniline

Received: June 16, 2011
Revised: July 23, 2011
Published: August 03, 2011

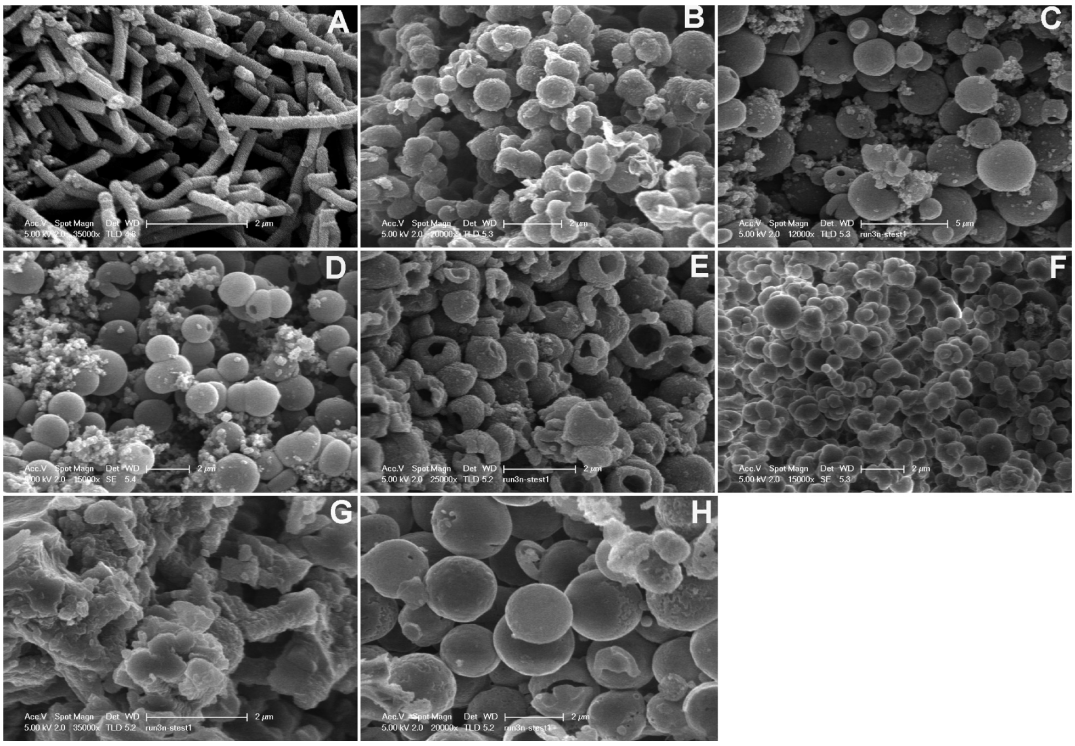

Figure 1. SEM images of the polymers synthesized in the presence of CSA: (A) PANI; (B) poly(*N*-methylaniline); (C) poly(*o*-toluidine); (D) poly(*m*-toluidine); (E) poly(*o*-anisidine); (F) poly(*m*-anisidine); (G) poly(*o*-phenetidine); (H) poly(*m*-phenetidine). The scale bar is 2 μm except in image C in which the scale bar is 5 μm.

oligomer with phenazine units produced in the early stages of oxidation (pH >4) serve as starting template sites for the future nucleation of PANI tubes. As pH decreases, the oligomers with phenazine units easily crystallize to produce one−dimensional structures and crystalline offshoots on the body of the amorphous precipitates. These crystalline offshoots serve as templates initiating the growth of nanotubes. The diameter of the offshoots determines the inner diameter of the future nanotubes. In this proposal, the formation of phenazine structures which are able to produce columnar aggregates by $\pi-\pi$ electron interactions plays a key role in the formation of PANI nanotubes. More recently, Zujovic et al. suggested that curling or rolling of nanosheets of polyaniline oligomers to form smooth oligomeric nanotubes in the first stage of oxidative polymerization which serve as templates in the followed polymerization of aniline at lower pH to form the PANI nanotubes.[22,23] Ding et al. reported that the formation of intermediate aggregates in the early stage of polymerization affects the morphologies of PANI nanomaterial, leading to either tubular or rod structures with striated growth and rough surfaces.[24]

Although the formation mechanism of PANI nanotubes is still open for discussion, a general sense from published work[7,15,19,25,26] is that the intermediates formed in the early stage of polymerization plays a key role in the formation of PANI nanotubes. To date, attempts to purify and identify the intermediates have proven to be a great challenge due to their high reactivity, polarity, and tendency for protonation and hydrogen bonding among the imine and amine groups in the oligomers.[27,28] In this work, we systematically investigated the morphologies of polymers prepared by using aniline and methyl-, methoxy-, or ethoxy-substituted aniline under the same experimental conditions. Because of the substitution at *o*-, *m*-, or *N*-positions of aniline, the oligomers produced in the early stage of aniline oxidation could not be formed. By examining the morphologies of oxidative products of substituted anilines, we obtained an insight into the formation mechanism of PANI nanotubes from a hitherto unexplored angle, as well as evaluating the nano/micro-structures of PANI derivatives.

EXPERIMENTAL SECTION

Materials. Aniline, *N*-methylaniline, *o*,*m*-toluidine, *o*,*m*-anisidine, *o*,*m*-phenetidine, 10-camphorsulfonic acid (CSA), and ammonium persulphate (APS) were obtained from Sigma-Aldrich. Aniline and its derivatives were distilled under vacuum before use. The other chemicals were purchased from the local suppliers and used without further purification.

Synthesis of PANI and Its Derivatives with Nano-/Micro-structures. The synthesis of polymers is according to refs 5 and 8. In general, 2 mmol of aniline or other monomers was dissolved in 10 mL of Milli-Q water containing 2 mmol of 10-camphorsulfonic acid (CSA). Then the solution was cooled in a refrigerator at 2−5 °C for 30 min, followed by the addition of 5 mL of precooled APS solution (0.4 M). The mixture was kept to react at 2−5 °C for 16 h. The precipitates collected were first washed several times with Milli-Q water, and then quick washed with methanol. Finally, the product was dried at 40 °C under vacuum for 24 h.

Characterization. The images of polymers morphologies were taken by using a Philips XL30S field emission scanning electron microscope (SEM). The UV−vis absorption spectra of the polymers dissolved in *m*-cresol were recorded by using a Shimadzu UV1700 UV−vis spectrophotometer. The FTIR spectra of polymers were measured on KBr pellets by means of a Perkin-Elmer 1600 FTIR spectrophotometer. Raman spectra in the range of 200−2000 cm^{-1} were collected from

Table 1. Summary of Morphological Characteristics of PANI and Its Derivatives

monomer	morphology of polymer	diameter (μm) outer (n = 20)	diameter (μm) inner (n = 5)	hole on surface?
aniline	nanotube	0.25 ± 0.09	0.024 ± 0.005	
N-methylaniline	hollow sphere	0.85 ± 0.45	0.59 ± 0.03	no
o-toluidine,	hollow sphere	2.5 ± 0.6	2.4 ± 0.5	yes
m-toluidine,	hollow sphere	1.6 ± 0.3	1.5 ± 0.2	yes
o-anisidine	hollow sphere	1.1 ± 0.3	0.8 ± 0.3	yes
m-anisidine	solid sphere	0.79 ± 0.42		no
o-phenetidine	granule			
m-phenetidine	hollow sphere	2.0 ± 0.3	1.6 ± 0.4	yes

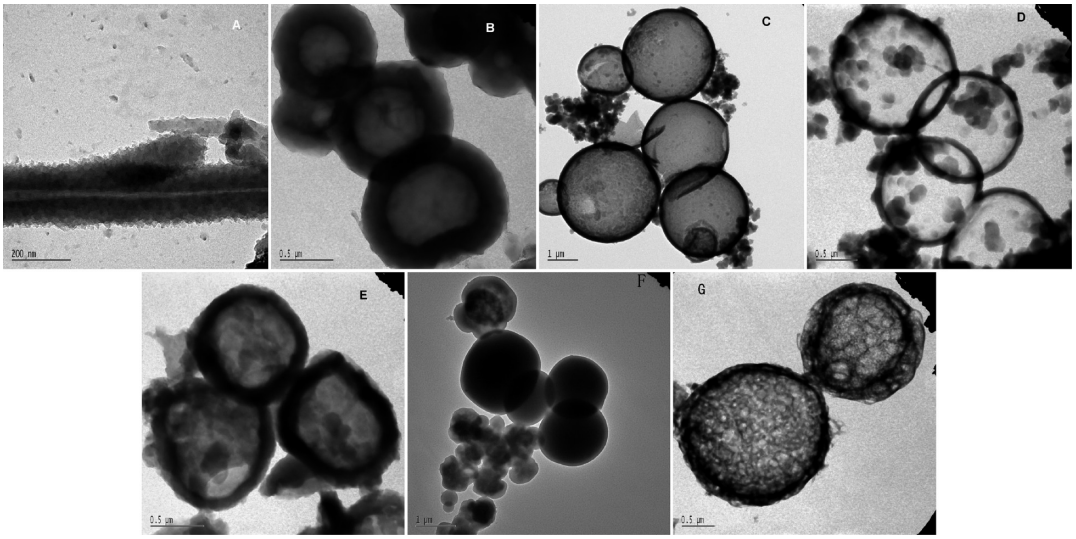

Figure 2. TEM images of the polymers synthesized in the presence of CSA: (A) PANI; (B) poly(*N*-methylaniline); (C) poly(*o*-toluidine); (D) poly(*m*-toluidine); (E) poly(*o*-anisidine); (F) poly(*m*-anisidine); (G) poly(*m*-phenetidine).

polymer powder samples using a Renishaw microscope (RM-1000) with 785 nm (red) laser excitation.

RESULTS AND DISCUSSION

In the presence of 10-camphorsulfonic acid (CSA), aniline or substituted anilines were oxidized in aqueous solution by using ammonium persulfate (APS) as an oxidant at 2−5 °C. The morphologies of obtained polymers are shown in Figure 1 and summarized in Table 1. Under experimental conditions used, the oxidation of aniline produced PANI nanotubes (Figure 1A) with an outer diameter of ∼250 nm. On the contrary, polymerization of aniline derivatives produces microspheres, except in the case of *o*-phenetidine whose polymer showed irregular morphology without microspheres or nanotubes (Figure 1G). In the case of methyl substituted aniline (*o*-toluidine and *m*-toluidine, Figure 1, parts C and D, respectively), relatively uniform microspheres of poly(*o*-toluidine) and poly(*m*-toluidine) were formed with an average outer diameter of 2.5 ± 0.6 μm and 1.6 ± 0.3 μm (n = 20), respectively. Holes or openings are clearly visible on the surface of microspheres of both polymers, which indicates the microspheres are hollow. If one proton of amino functionality is substituted by a methyl group (*N*-methylaniline), the morphology of the corresponding polymer was found to be microspherical with an average outer diameters of 0.85 ± 0.45 μm (n = 20) (Figure 1 B). For poly(*o*-anisidine) and poly(*m*-anisidine), the average outer diameters of microspheres are 1.1 ± 0.3 μm and 0.79 ± 0.42 μm (n = 20), respectively. It can be clearly seen from the openings on the surface of poly(*o*-anisidine) microspheres that they are hollow, while there are no visible holes or openings on the surface of poly(*m*-anisidine). For ethoxy group substituted aniline, poly(*o*-phenetidine) shows granular morphology (Figure 1G), while poly(*m*-phenetidine) forms nice microspheres with an average outer diameters of 2.0 ± 0.3 μm (n = 20), as well as small holes on the surface (Figure 1H).

Figure 2 presents TEM images of the prepared polymers except poly(*o*-phenetidine). The average inner diameter of PANI nanotubes is 24 ± 5 nm (n = 5), as summarized in Table 1. TEM images of poly(*o*-toluidine) and poly(*m*-toluidine) (Figure 2C and D) further confirmed that both microspheres were hollow. The average inner diameters of hollow microspheres are 2.4 ± 0.5 μm and 1.5 ± 0.2 μm (n = 5) for poly(*o*-toluidine) and poly(*m*-toluidine), respectively. The microspheres of poly(*N*-methylaniline) are also hollow, as shown in Figure 2B. Compared with poly(*o*-toluidine) and poly(*m*-toluidine), the shell thickness of poly(*N*-methylaniline) microspheres is much larger. For poly(*o*-anisidine) and poly(*m*-anisidine), it is interesting that

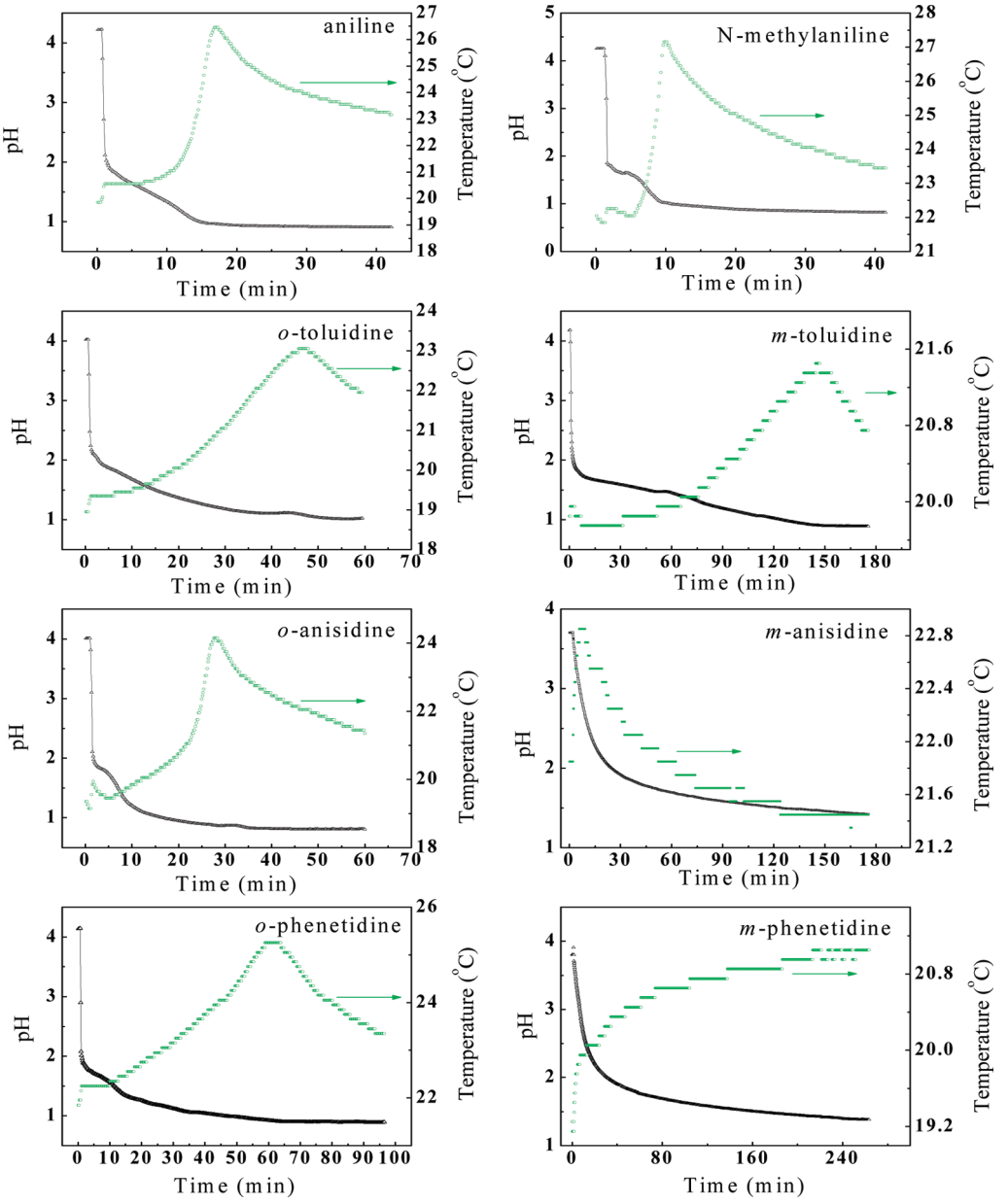

Figure 3. pH and temperature profiles during the oxidation of 0.2 M aniline and its derivatives by using APS as the oxidant.

poly(*o*-anisidine) microspheres are hollow (Figure 2E), while poly(*m*-anisidine) microspheres are solid. The reason is not clear and we presume it is related to the ability of *m*-anisidine to form micelles with CSA. Because of the irregular morphology of poly(*o*-phenetidine), it was not characterized by TEM. As shown in Figure 2F, poly(*m*-phenetidine) microspheres are also hollow.

From the SEM and TEM results, it is obvious that under the identical experimental conditions, only aniline produced nanotubes in the course of oxidative polymerization. As proposed, there are many factors affecting the morphology of PANI, such as the acidity of reaction medium, temperature, concentration of the reactants and their ratio; however, the acidity of the reaction medium plays the key role in the self-assembly formation of PANI nanotubes.[15,29,30] When APS is used as the oxidant, sulfuric acid is a byproduct due to the release of protons from the oxidation of aniline and its derivatives, which causes an increase in the acidity of reaction medium in the course of polymerization. Oxidation of anline and its derivatives is also an exothermic reaction, which results in an increase in the temperature of the reaction medium during the polymerization. In order to distinguish the contribution of pH and the temperature changes to the differences in the morphologies of PANI and its derivatives, we monitored the time-dependence of pH and temperature in the reaction medium in the course of polymerization. The results are presents in Figure 3. For aniline, pH drops dramatically after the addition of APS and the temperature increases correspondingly. After pH falls to 2, the decrease of pH slows down and the temperature stays constant. When pH is lower than 1.5, the decrease of pH is concomitant with a large tmeperature increase in the reaction medium. As it is well-known, aniline is a weak base (pK_a 4.65 at 25 °C). The pH value of aniline

dx.doi.org/10.1021/ma201350m |*Macromolecules* 2011, 44, 6899–6907

Scheme 1. Proposed Oligomers Structures Formed in the Initial Oxidation of Aniline

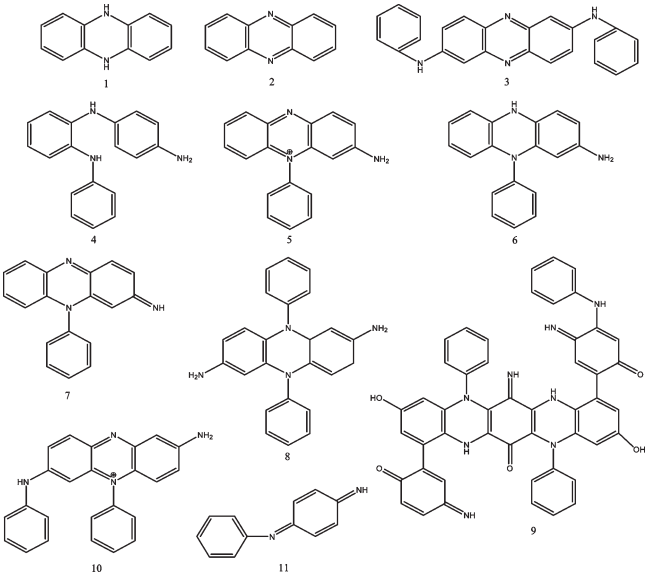

solution in the presense of CSA is 4.2, indicating that the solution contains both neutral aniline molecules and anilinium cations. After the addition of APS, the neutral aniline molecules are first oxidized to oligomers, because they are much easier to be oxidized than anilinium cations in which the electron pair on nitrogen is localized.[31] The oxidation of neutral aniline molecules corresponds to the first exothermic process as shown in Figure 3. With the decrease of pH, the equilibrium between neutral aniline and anilinim cations shifts in favor of the latter species. Because of the difficult oxidation of anilinim cations and the decrease of neutral aniline molecule fraction in the reaction medium, the reaction considerably slows down, as illustrated by the unchanged temperature and slow decrease of pH. This stage is known as the athermal induction period in the synthesis of PANI in acidic media.[32,33] The second heat evolution wave starts at pH of around 1.5. In this stage, pernigraniline intermidiates are protonated and anilinium cations can now be easily oxidized to grow the polymer chains in the protonated pernigraniline form.[19] The reaction eventually stops when all availabe monomer is consumed; pH at that stage is approximatelly 1.0.

The pK_a of aniline derivatives used is in the range from 4 to 5. In the prescence of 0.13 M CSA, the neutral and protonated molecules coexist, so the oxidation of aniline derivatives shows similar behaviors as that of aniline except *m*-anisidine and *m*-phenetidine, as illustrated in Figure 3. For example, the oxidation of *N*-methylaniline has two exotherimic processes, separated by an induction period. While, in the case of the oxidation of *m*-anisidine, the temperature quickly increased after the addition of APS, then kept on falling. For *m*-phenetidine, the temperature kept on increasing with the slow decrease of pH which indicates a lower rate of polymer chain growth.

The oxidation of neutral aniline produces oligomers containing both *ortho* and *para* coupling products, whose possible structures proposed in the literatures are given in Scheme 1.[19,27,28,34] Most of proposed oligomers contains phenazine parent structure which is formed through the oxidative cyclization of *ortho*-coupled aniline units.[35,36] The phenazine-like oligomers with relatively flat molecular structures are hydrophobic and able to

Table 2. Weight-Average Molecular Weight (M_w), Number-Average Molecular Weight (M_n), and Polydispersity Index (PDI) of PANI and its derivatives

	M_w	M_n	PDI
PANI	77 000	41 000	1.9
poly(*N*-methylaniline)	48 000	23 000	2.1
poly(*o*-toluidine)	62 000	22 000	2.8
poly(*m*-toluidine)	40 000	11 000	3.6
poly(*o*-anisidine)	48 000	14 000	3.4
poly(*m*-anisidine)	12 000	2900	4.1
poly(*o*-phenetidine)	29 000	6800	4.3
poly(*m*-phenetidine)	19 000	3900	4.9

produce one-dimensional stacks stabilized by $\pi-\pi$ interactions. The produced stacks are critical for the formation of nanotubes, because they act as a template for the subsequent growth of PANI chain into the aqueous phase producing the wall of nanotubes at lower pH level, as proposed by Stejskal et al.[15,19] Aniline derivatives, although their oxidation behavior is similar to that of aniline, cannot produce the oligomers with phenazine-like structures at the high pH level due to the presence of substitued groups at the ortho and meta position. This explains the different morphologies of PANI and its derivatives. Because of the lack of the stacking template, PANI derivatives can not form the nanotubes, or other one-dimension almorphologies such as nanofibers, which in turn confirms that the oligomers with phenazine-like structures formed at high pH are essential for the formation of PANI nanotubes.

Kaner's group reported the preparation of substituted polyaniline nanofibers, such as poly(*o*-ethylaniline), poly(*N*-ethylaniline), poly(*o*-chloroaniline), and poly(*o*-methoxyaniline).[37−39] According to their studies, the addition of initiator *p*-phenylenediamine is essential for the formation of polymer nanofibers. The authors suggest that the initiator accelerates the polymerization rate which favors homogeneous nucleation over heterogeneous nucleation and the initiator molecules can serve as the nucleation center for the polymer chain growth.[37,38] In our experiments, the reaction kinetics of *N*-methylaniline and *o*-anisidine is very close to that of aniline, as illustrated by the time-dependence of pH and temperature (Figure 3), however the morphologies of the final products are different. We speculate that the oxidation of *p*-phenylenediamine also produces phenazine containing structures,[40,41] which can form one-dimensional stacks and act as the templates to guide the formation of substituted polyaniline nanofibers. The combination of Kaner's results[37−39] and ours suggest that the oligomers with phenazine structures are essential for the formation of PANI with one-dimensional nanostructures.

For PANI derivatives, the substituent groups and position also affect the morphologies. Compared with methoxyl substituted aniline, methyl substitution results in more uniform polymer microspheres (Figure 1C and D). Increasing the length of substituted group produces larger microsphere, such as in the case of poly(*m*-anisidine) and poly(*m*-phenetidine). For the same substitution group, *ortho*-substitution results in larger spheres than *meta*-substitution and N-substitution. The wall thickness of PANI derivatives microspheres is also affected by the substituent groups and position, since the substituents are known to affect the reactivity of monomers and reduce the degree of polymerization.[37,42] For example, the sequence of wall thickness in terms of methyl substituted polymers is following:

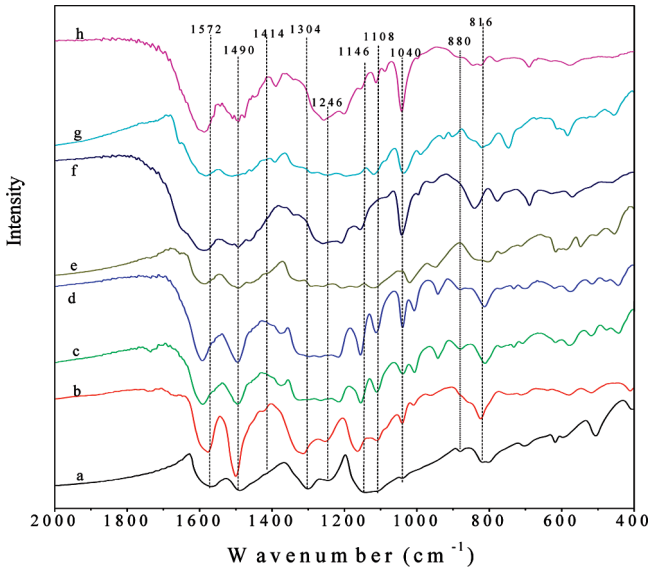

Figure 4. FT-IR spectra of polymers synthesized in the presence of CSA: (a) PANI; (b) poly(*N*-methylaniline); (c) poly(*o*-toluidine); (d) poly(*m*-toluidine); (e) poly(*o*-anisidine); (f) poly(*m*-anisidine); (g) poly(*o*-phenetidine); (h) poly(*m*-phenetidine).

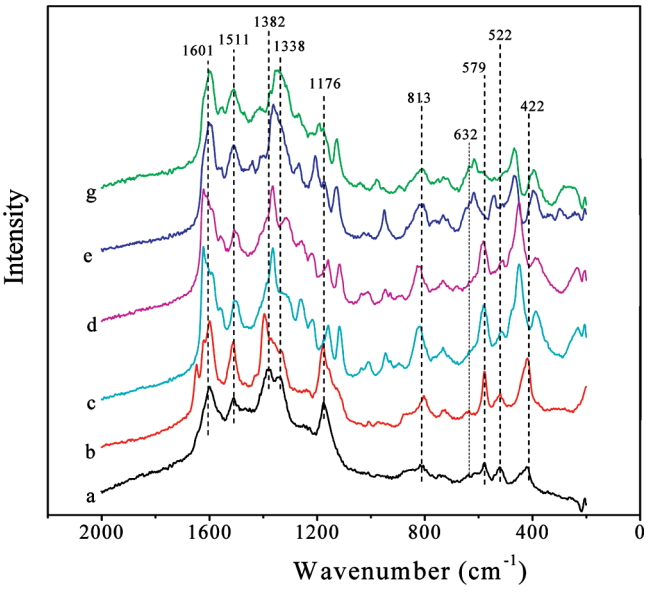

Figure 5. Raman spectra of polymers synthesized in the presence of CSA: (a) PANI; (b) poly(*N*-methylaniline); (c) poly(*o*-toluidine); (d) poly(*m*-toluidine); (e) poly(*o*-anisidine); (g) poly(*o*-phenetidine).

poly(*N*-methylaniline) > poly(*o*-toluidine) > poly(*m*-toluidine). From Figure 3, it can be seen that the polymerization rate sequence of these three monomers is same as that of the wall thickness, which implies that a faster polymerization rate results in a thicker wall. In order to evaluate their contribution to the wall thickness, the molecular weights of PANI and its derivatives were measured by gel permeation chromatography using NMP/LiBr as the eluant and the results are given in Table 2. In general, the molecular weight of PANI derivatives is smaller than that of PANI because of the substitution. The molecular weight of *ortho*-substituted PANI is larger than that of *meta*-substituted PANI due to the large steric hindrance to the polymeric chain growth in *para*-position when *meta*-position is substituted. Coming back to methyl substituted polymers, the molecular weight of poly(*o*-toluidine) was larger than that of poly(*N*-methylaniline), but the wall of poly(*o*-toluidine) was thinner, which indicates that the polymerization rate contributes more to the wall thickness than the length of polymer chain. This result also implies that the polymer chain did not grow vertically, otherwise the longer polymer chains should result in a thicker wall.

The molecular structures of PANI and its derivatives are characterized by FTIR and Raman spectroscopy. The FTIR spectra are shown in Figure 4. Curve a in Figure 4 gives a typical spectrum of PANI nanotubes. The 1572 cm^{-1} band is characteristic of quinine diimine ring-stretching deformation, while 1490 cm^{-1} band indicates benzonoid diamine ring stretching.[43] The relative intensities of these two bands imply the structure of polymer backbone is close to the emeraldine form. The 1304 cm^{-1} band corresponds to C−N stretching in the proximity of quinoid rings. The 1146 cm^{-1} band is assigned to either $-NH^+$ stretching modes of the doped state[9] or to the high degree of electron delocalization of the doped state.[44] The band located at 1040 cm^{-1} is associated with aryl-S group which may come from the sulfonation of PANI or the dopant CSA. Stejskal et al suggests that the 1414 cm^{-1} band is the characteristic vibrational frequency of phenazine-like structures formed at the early oxidation stage of aniline.[19] However, this band is not obvious in FTIR spectrum of the final product of PANI nanotubes (Figure 4, curve a), same as what we found in our previous work.[4,5] This is possibly because the oligomer template with phenazine-like structures dissolves after being protonated at the low pH stage in the course of polymerization, which has been suggested by Stejskal et al[45] and Ding et al[46] or are fully covered with PANI obtained at later stages of polymerization. The FTIR spectra of PANI derivatives are more complex than that of PANI, as shown in Figure 4 (curves b−h). The characteristic band of phenazine-like structures at 1414 cm^{-1} is not observed in any of these spectra. This is reasonable because the substitution at *ortho*-, *meta*- and N- positions will hinder the formation of phenazine-like structures. The relative intensity of 1146 cm^{-1} band of PANI derivatives assigned to $-NH^+$ stretching vibration modes is lower than that of PANI. This result implies that the conductivity of PANI derivatives is lower. It is notable that the 1040 cm^{-1} band in the spectra of PANI derivatives is much stronger than that of PANI. This is probably due to the easy sulfonation of aniline derivatives substituted with electron-donating groups.

Raman spectra were measured by using a laser with an excitation wavelength of 785 nm and are presented in Figure 5. Because of the large background signal, the Raman spectra of poly(*m*-anisidine) and poly(*m*-phenetidine) were not obtained. For PANI, several characteristic dominating bands are observed. The C−C stretching vibration of benzenoid and quinoid rings locates at 1601 and 1382 cm^{-1}, respectively.[47,48] The 1511 cm^{-1} band is due to the C═N stretching mode of quinoid rings. The band at 1338 cm^{-1}, assigned to the $C-N^+$ stretching vibration, clearly shows that PANI nanotubes are in a doped state. The bands at 813 and 422 cm^{-1} are related to the C−H deformation. The bands at 579 and 522 cm^{-1} were earlier ascribed to the amine deformation and C−N−C torsion, respectively.[47] The band at 632 cm^{-1} is due to the C−S stretching vibration or SO_3 deformation vibration.[49] The dominating bands in the Raman spectra of PANI derivatives are similar to those of PANI, as show in Figure 5 (curves b−g). However, the relative intensity of the

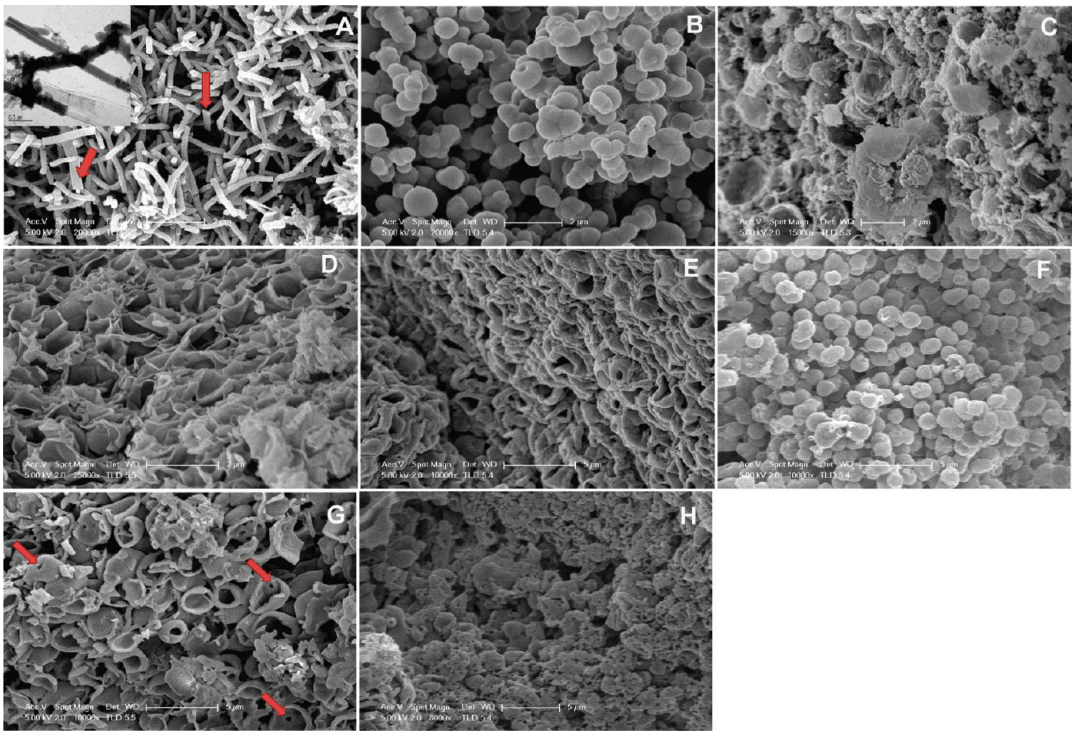

Figure 6. SEM images of the polymers synthesized in absence of CSA: (A) PANI; (B) poly(*N*-methylaniline); (C) poly(*o*-toluidine); (D) poly(*m*-toluidine); (E) poly(*o*-anisidine); (F) poly(*m*-anisidine); (G) poly(*o*-phenetidine); (H) poly(*m*-phenetidine). Inset: TEM of PANI nanotubes and nanorods.

band around 1338 cm^{-1}, assigned to $C-N^+$ stretching vibration, in PANI derivatives is lower than that of PANI, which is in consistent with the FTIR results. The much stronger band at ~632 cm^{-1} in the spectra of PANI derivatives also suggests the easy sulfonation of aniline derivatives, which agrees with the result ofFTIR spectroscopy. The 1415 cm^{-1} band suggested to be a strong band associated with substituted phenazine segments by Stejskal et al[48] is also not observed in the spectra of PANI derivatives.

In order to evaluate the contribution of CSA to the morphologies of PANI and its derivatives, we prepared these polymers without the addition of CSA. The SEM results are given in Figure 6. It is clear that PANI nanotubes can still be obtained in the absence of CSA. However, nanorods and some nanobelts of PANI are observed, as shown in the insect and indicated by the arrows in Figure 6A, respectively. This result illustrates that the presence of CSA is not crucial for the formation of PANI nanotubes, which can be explained by the fact that aniline solution is basic and the oxidation of aniline in such solution even favors the formation phenazine-like oligomers. For PANI derivatives, the morphologies are quite different without the addition of CSA, except poly(*N*-methylaniline) and poly(*m*-anisidine) which are still in a form of microspheres. In the case of poly(*o*-toluidine) and poly(*m*-toluidine), broken egg shell, and petallike morphologies are produced, respectively. For poly(*o*-anisidine), crowded flat spheres are formed. Poly(*o*-phenetidine) prepared in the absence of CSA forms imperfect microspheres, which are quite different from the morphology obtained when prepared in the presence of CSA. Finally, poly(*m*-phenetidine) morphology is of porous granules. These results imply that CSA plays an important role in the well-defined microsphere formation of PANI derivatives under our experimental conditions.

As seen from Figure 6, the oxidation of most PANI derivatives did not produce uniform microsphere in the absence of CSA, but they do show a tendency to the formation of hollow microspheres. The mechanism for the formation of such hollow microsphere is still open for discussion. At present, a suggested mechanism is that aniline derivatives form micelle droplets in aqueous solution in the presence of organic acid which act as templates for the polymerization.[11,50,51] Guo et al[51] proposed that aniline derivatives formed droplets when they were added to water due to the presence of a hydrophilic $-NH_2$ group and hydrophobic $-C_6H_4$ and $-CH_3$ groups. After the addition of APS, which is hydrophilic, the polymerization took place at the interface of water/droplet to produce small hollow nanostructures. Because of the larger size of final microspheres than that of droplets,[51,52] the authors suggested that these nanostructures originated from the droplets fusing and aggregating to form the final large hollow spheres.[51] However, what drives these nanostructures to fuse or aggregate to large hollow spheres and why the inner diameter is larger than that of droplet are still in question. As discussed before, the oxidation of aniline derivatives at high pH produces oligomers. These oligomers do not contain phenazine-like structures and are difficult to form one-dimensional structure. So it is reasonable to expect that these hydrophobic oligomers self-assemble at the interface of water/droplet and act as the template for the formation of the final hollow microspheres. The heat released during the oxidation of aniline derivatives will increase the local temperature of droplets, which results in the swelling of droplets or fusing of droplets. Another factor contributing to the swelling of droplets may come from the osmotic pressure, because the pH drop during the oxidation causes the monomer inside the droplets to gradually protonate and attract water to the interior to dissolve formed cations. The swelling or fusing of the

droplets affects the assembly of oligomers to form a template for the formation of micrometers-sized hollow spheres during the polymer chain propagation stage. So the different stability of aniline derivatives droplets formed and the exothermal oxidation rate correspond to the different morphologies of PANI derivatives. In the cases of poly(*N*-methylaniline) and poly(*m*-anisidine) which form relatively uniform hollow spheres (Figure 6, part B and F), the exothermal process during the polymerization is shorter than that of others, as illustrated in Figure 3. This short exothermal process benefits the maintenance of droplets and assembly of oligomers, resulting in the formation of the final well-defined microspheres. On the other hand, in the presence of CSA, which is a surfactant and also cause partial protonation of the monomers, the droplets are more stable which benefits the self-assembly of oligomers at the interface of water/droplets during the polymer chain propagation. So the oxidation of most aniline derivatives produces nice hollow microspheres (Figure 1).

It can be clearly seen from Figure 1 and Figure 6 that there are openings or holes on the surface of some PANI derivatives such as poly(*o*-toluidine), poly(*m*-toluidine) and poly(*m*-phenetidine). Guo et al. suggest that the formation of holes is due to the diffusion of monomers to outside.[51] However, that cannot answer the question why the monomers are not oxidized to form a shell when they diffuse to APS-rich exterior. We believe that the swelling of the droplets and the protonation of monomers will attract water and water-soluble components into the interior. The flux of water and water-soluble components is maintained during the whole polymerization process, resulting in the formation of openings or holes on the surfaces. From Figure 6G, the hole can be clearly seen as indicated by the arrows although the morphology is that of broken microspheres. This indicates the holes were probably formed at the initial oxidation stage of aniline derivatives. During polymer chain propagation process, the microspheres rupture due to the heat released or osmotic pressure. The existence of the holes on these broken microspheres' surface further supports our proposed mechanisms for the formation of hollow microsphere and hole.

CONCLUSIONS

In this work, we synthesized PANI and its derivatives through the chemical oxidation of corresponding monomers in the presence and absence of CSA. The oxidation of aniline in both cases produces nanotubes, while the oxidation of aniline derivatives does not produce such one-dimensional nanostructures under the same experimental conditions. These results illustrate the oligomers with phenazine-like structures produced at the initial oxidation of aniline are crucial for the formation of PANI nanotubes.

For aniline derivatives, the chemical oxidation in the presence of CSA mainly produces hollow microspheres. The role of CSA is mainly to stabilize the droplets of aniline derivatives during oxidation, resulting in the formation of the well-defined hollow microspheres. In the absence of CSA, the main factors to define the polymer morphology are stability of droplets and the rate of exothermal reaction. The fast exothermal reaction benefits the formation of microspheres. We also suggest that the hole on the surface of microspheres forms at the initial oxidation stage and are maintained by the flux of water and water-soluble components in the course of polymerization.

AUTHOR INFORMATION

Corresponding Author

*E-mail: (H.P.) hpeng@ee.ecnu.edu.cn; (J.T.-S.) j.travas-sejdic@auckland.ac.nz.

ACKNOWLEDGMENT

The authors gratefully acknowledge Foundation for Research, Science and Technology of New Zealand, National Natural Science Foundation of China (No. 60976004), Shanghai Pujiang Program, PCSIRT and the Talent Program of East China Normal University for financial support.

REFERENCES

(1) Shirakawa, H.; Louis, E. J.; MacDiarmid, A. G.; Chiang, C. K.; Heeger, A. J. *J. Chem. Soc., Chem. Commun.* **1977**, *16*, 578–80.
(2) Wan, M. *Encycl. Nanosci. Nanotechnol.* **2004**, *2*, 153–169.
(3) Zhang, L.; Peng, H.; Kilmartin, P. A.; Soeller, C.; Tilley, R.; Travas-Sejdic, J. *Macromol. Rapid Commun.* **2008**, *29* (7), 598–603.
(4) Zhang, L.; Peng, H.; Zujovic, Z. D.; Kilmartin, P. A.; Travas-Sejdic, J. *Macromol. Chem. Phys.* **2007**, *208* (11), 1210–1217.
(5) Zhang, L.; Peng, H.; Hsu, C. F.; Kilmartin, P. A.; Travas-Sejdic, J. *Nanotechnology* **2007**, *18* (11), 115607/1–115607/6.
(6) Wan, M. X.; Shen, Y. Q.; Huang, J. Chinese patent No. 98109916.5, 1998.
(7) Wan, M. *Adv. Mater.* **2008**, *20* (15), 2926–2932.
(8) Zhang, L.; Wan, M. *Nanotechnology* **2002**, *13* (6), 750–755.
(9) Zhang, L.; Zujovic, Z. D.; Peng, H.; Bowmaker, G. A.; Kilmartin, P. A.; Travas-Sejdic, J. *Macromolecules* **2008**, *41* (22), 8877–8884.
(10) Konyushenko, E. N.; Stejskal, J.; Sedenkova, I.; Trchova, M.; Sapurina, I.; Cieslar, M.; Prokes, J. *Polym. Int.* **2006**, *55* (1), 31–39.
(11) Wei, Z.; Wan, M. *Adv. Mater.* **2002**, *14* (18), 1314–1317.
(12) Zhang, L.; Wan, M. *Adv. Funct. Mater.* **2003**, *13* (10), 815–820.
(13) Zhang, Z.; Wei, Z.; Wan, M. *Macromolecules* **2002**, *35* (15), 5937–5942.
(14) Wei, Z.; Zhang, Z.; Wan, M. *Langmuir* **2002**, *18* (3), 917–921.
(15) Stejskal, J.; Sapurina, I.; Trchova, M.; Konyushenko, E. N.; Holler, P. *Polymer* **2006**, *47* (25), 8253–8262.
(16) Lu, X.; Mao, H.; Chao, D.; Zhang, W.; Wei, Y. *Macromol. Chem. Phys.* **2006**, *207* (22), 2142–2152.
(17) Chiou, N.-R.; Lee, L. J.; Epstein, A. J. *Chem. Mater.* **2007**, *19* (15), 3589–3591.
(18) Ding, H.; Shen, J.; Wan, M.; Chen, Z. *Macromol. Chem. Phys.* **2008**, *209* (8), 864–871.
(19) Stejskal, J.; Sapurina, I.; Trchova, M.; Konyushenko, E. N. *Macromolecules* **2008**, *41* (10), 3530–3536.
(20) Sapurina, I.; Stejskal, J. *Polym. Int.* **2008**, *57* (12), 1295–1325.
(21) Stejskal, J.; Sapurina, I.; Trchová, M. *Prog. Polym. Sci.* **2010**, *35* (12), 1420–1481.
(22) Zujovic, Z. D.; Laslau, C.; Bowmaker, G. A.; Kilmartin, P. A.; Webber, A. L.; Brown, S. P.; Travas-Sejdic, J. *Macromolecules* **2010**, *43* (2), 662–670.
(23) Laslau, C.; Zujovic, Z.; Travas-Sejdic, J. *Prog. Polym. Sci.* **2010**, *35* (12), 1403–1419.
(24) Ding, Z. F.; Yanag, D. L.; Currier, R. P.; Obrey, S. J.; Zhao, Y. S. *Macromol. Chem. Phys.* **2010**, *211* (6), 627–634.
(25) Huang, Y. F.; Lin, C. W. *Synthet. Met.* **2009**, *159* (17−18), 1824–1830.
(26) Ding, Z.; Yang, D.; Currier, R. P.; Obrey, S. J.; Zhao, Y. *Macromol. Chem. Phys.* **2010**, *211* (6), 627–634.
(27) Kriz, J.; Starovoytova, L.; Trchova, M.; Konyushenko, E. N.; Stejskal, J. *J. Phys. Chem. B* **2009**, *113* (19), 6666–6673.
(28) Ding, Z.; Sanchez, T.; Labouriau, A.; Iyer, S.; Larson, T.; Currier, R.; Zhao, Y.; Yang, D. *J. Phys. Chem. B* **2010**, *114* (32), 10337–10346.

(29) Laslau, C.; Zujovic, Z. D.; Zhang, L.; Bowmaker, G. A.; Travas-Sejdic, J. *Chem. Mater.* **2009**, *21* (5), 954–962.
(30) Wan, M. *Macromol. Rapid Commun.* **2009**, *30* (12), 963–975.
(31) Hendrickson, J. B.; Cram, D. J.; Hammond, G. S. *Organic Chemistry*; McGraw-Hill: New York, 1970; p 1279 pp.
(32) Stejskal, J.; Gilbert, R. G. *Pure Appl. Chem.* **2002**, *74* (5), 857–867.
(33) Pud, A. A.; Noskov, Y. V.; Kassiba, A.; Fatyeyeva, K. Y.; Ogurtsov, N. A.; Makowska-Janusik, M.; Bednarski, W.; Tabellout, M.; Shapoval, G. S. *J. Phys. Chem. B* **2007**, *111* (9), 2174–2180.
(34) Surwade, S. P.; Dua, V.; Manohar, N.; Manohar, S. K.; Beck, E.; Ferraris, J. P. *Synthet. Met.* **2009**, *159* (5−6), 445–455.
(35) Ciric-Marjanovic, G.; Konyushenko, E. N.; Trchova, M.; Stejskal, J. *Synthet. Met.* **2008**, *158* (5), 200–211.
(36) Ciric-Marjanovic, G.; Trchova, M.; Stejskal, J. *Int. J. Quantum Chem.* **2007**, *108* (2), 318–333.
(37) Tran, H. D.; Norris, I.; D'Arcy, J. M.; Tsang, H.; Wang, Y.; Mattes, B. R.; Kaner, R. B. *Macromolecules* **2008**, *41* (20), 7405–7410.
(38) Tran, H. D.; Kaner, R. B. *Chem. Commun.* **2006**, *37*, 3915–3917.
(39) Wang, Y.; Tran, H. D.; Kaner, R. B. *J. Phys. Chem. C* **2009**, *113* (24), 10346–10349.
(40) Cataldo, F. *Eur. Polym. J.* **1996**, *32* (1), 43–50.
(41) Zujovic, Z. D.; Wang, Y.; Bowmaker, G. A.; Kaner, R. B. *Macromolecules* **2011**, *44* (8), 2735–2742.
(42) Zaidi, N. A.; Foreman, J. P.; Tzamalis, G.; Monkman, S. C.; Monkman, A. P. *Adv. Funct. Mater.* **2004**, *14* (5), 479–486.
(43) Kang, E. T.; Neoh, K. G.; Tan, K. L. *Prog. Polym. Sci.* **1998**, *23* (2), 277–324.
(44) Neoh, K. G.; Kang, E. T.; Tan, K. L. *Polymer* **1993**, *34* (18), 3921–3928.
(45) Janosevic, A.; Ciric-Marjanovic, G.; Marjanovic, B.; Holler, P.; Trchova, M.; Stejskal, J. *Nanotechnology* **2008**, 135606.
(46) Ding, Z. F.; Currier, R. P.; Zhao, Y. S.; Yang, D. L. *Macromol. Chem. Phys.* **2009**, *210* (19), 1600–1606.
(47) Cochet, M.; Louarn, G.; Quillard, S.; Buisson, J. P.; Lefrant, S. *J. Raman Spectrosc.* **2000**, *31* (12), 1041–1049.
(48) Ciri-Marjanovic, G.; Trchova, M.; Stejskal, J. *J. Raman Spectrosc.* **2008**, *39* (10), 1375–1387.
(49) Panicker, C. Y.; Varghese, H. T.; Anto, P. L.; Philip, D. *J. Raman Spectrosc.* **2006**, *37* (8), 853–857.
(50) Zhang, L.; Wan, M.; Wei, Y. *Macromol. Rapid Commun.* **2006**, *27* (11), 888–893.
(51) Han, J.; Song, G.; Guo, R. *Adv. Mater.* **2006**, *18* (23), 3140–3144.
(52) Sui, J.; Zhang, L.; Peng, H.; Travas-Sejdic, J.; Kilmartin, P. A. *Nanotechnology* **2009**, *20* (41), 415606/1–415606/8.